Arch. Metall. Mater. **70** (2025), 3, 1181-1187

DOI: https://doi.org/10.24425/amm.2025.154465

HONG-GU LEE[1], AYEONG LEE[1], SU-GWAN LEE[1], CHAE-RYEONG KIM[1], JIN-CHUN KIM[1*], SANG-YONG SHIN[1]

MICROSTRUCTURE AND MECHANICAL PROPERTIES OF HIGH-STRENGTH TOOL STEELS

In this study, high-strength tool steel specimens based on AISI D2 with a C content of 1.6% or more were developed by adjusting alloying elements (C, Cr, Mo, and V). Specimens were manufactured through various heat treatments such as austenitizing, quenching, and tempering processes, and their microstructure and mechanical properties are analyzed. The hardness results varied significantly depending on the alloy composition and microstructural characteristics. For example, Fe3 with increased C and Mo contents and uniform martensite and carbide microstructure has the highest hardness (862 HV, 704 HV) both before and after tempering. Among the quenched specimens, the lowest hardness (661 HV) was observed in MD2, which had a standard AISI D2 composition and exhibited a microstructure that was fine in scale but non-uniform in distribution. Among the as-tempered specimens, the lowest hardness (581HV) was observed in Fe2, which had a relatively heterogeneous microstructure despite its increased Cr and Mo contents.

Keywords: High strength tool steel; Heat treatment process; AISI D2; Microstructure; Hardness

1. Introduction

The automotive industry is actively pursuing vehicle electrification and lightweighting. These trends have spurred growing interest in metal additive manufacturing (AM) as a promising approach to enhance market competitiveness.

Gear components used in power transmission systems require high dimensional precision, exceptional strength, and superior wear resistance. AISI D2, a high-carbon tool steel with excellent hardness and wear resistance, meets these demands. However, its application has been limited due to the difficulties of fabricating complex parts using conventional manufacturing methods. Given this background AM, which enables precise fabrication, has been proposed as a promising alternative for the production of AISI D2 components.

To enable the mass production of AISI D2 components using AM, it is essential to establish optimal alloy compositions and heat treatment conditions that can deliver the desired microstructure and mechanical properties. This study aims to design chemical composition of experimental alloys and appropriate heat treatment processes, and to investigate their effects on microstructure and mechanical properties.

AISI D2 exhibits high hardness but suffers from low toughness. To address this limitation, research efforts have focused on improving its toughness while preserving its hardness. Achieving a balance between hardness and toughness requires a heat treatment process, typically consisting of austenitizing, quenching, and tempering. [1] When quenching is performed after austenitizing, the martensitic transformation is accompanied by volume expansion, which induces residual stresses. The rapid cooling during quenching generates internal stresses that not only facilitate phase transformation but also promote the formation of nucleation sites for carbide precipitation during subsequent tempering. These stresses can enhance strength but may also increase brittleness. [2-5] To address this, tempering is typically applied to relieve internal stresses and improve toughness. Following tempering, secondary carbides precipitate due to the high carbon and alloying element content of the steel. [2,6-8] Tempering also reduces dislocation density and relieves quenching-induced stress, generally leading to a reduction in hardness. However, this hardness loss can be mitigated if retained austenite transforms into martensite and additional carbides precipitate during the tempering process.

[5] Against this background, heat treatment serves as a key approach to fine-tuning the mechanical properties of AISI D2 through controlled microstructural transformations.

[1] UNIVERSITY OF ULSAN, SCHOOL OF MATERIALS SCIENCE AND ENGINEERING, ULSAN, REPUBLIC OF KOREA

* Corresponding author: jckimpml@ulsan.ac.kr

2. Experimental

2.1. Preparation of specimens

Chemical composition of experimental alloys was designed by optimizing the contents of the main components – C, Cr, Mo, and V – as variables. Experimental alloys were manufactured using a Vacuum Plasma Melter.

TABLE1

Comparison of design and actual chemical composition (wt.%) of experimental alloy

	C	Cr	Mo	V	C	Cr	Mo	V
MD2	1.6	12	1	0.004	1.55	11.6	0.72	0.004
Fe1	1.6	12	1	1	1.57	11	0.89	0.92
Fe2	1.6	13	1.2	0.5	1.6	12.8	1.05	0.51
Fe3	2	12	1	1	2	11.9	0.97	0.99

MD2 was designed to maintain the characteristics of standard AISI D2. Fe1 had increased V content compared to standard AISI D2 steel, promoting the formation of V carbide. Fe2 was designed with higher Cr, Mo, and slightly increased V contents to induce a low-temperature transformation structure and carbide formation. Fe3 had elevated C, Cr, Mo, and V contents to achieve a similar low-temperature transformation structure and carbide formation.

2.2. Heat treatment of specimens

[1] The heat treatment process began with austenitizing the specimens at 1000°C for 45 minutes, followed by water quenching at 20°C for 5 minutes. Tempering was then performed in two cycles at 540°C for 1 hour each, with air cooling to room temperature between cycles. This double tempering was applied because the high carbon content increases the stability of retained austenite, making a single tempering cycle insufficient for effective phase transformation.

Based on the heat treatment conditions, the specimens were categorized into three groups: as-received, as-quenched, and as-tempered.

2.3. Analysis of microstructure and mechanical properties

All specimens were polished to 1 μm finish and then etched in a nital solution for 50 seconds.

The phase fraction expressed as area percent and average size of each phase in the specimen microstructures were analyzed. The reported values for each specimen were based on at least 8 measurements in different fields at 500× magnification. Microstructure analysis was performed on specimens using an optical microscope (OM) and scanning electron microscope

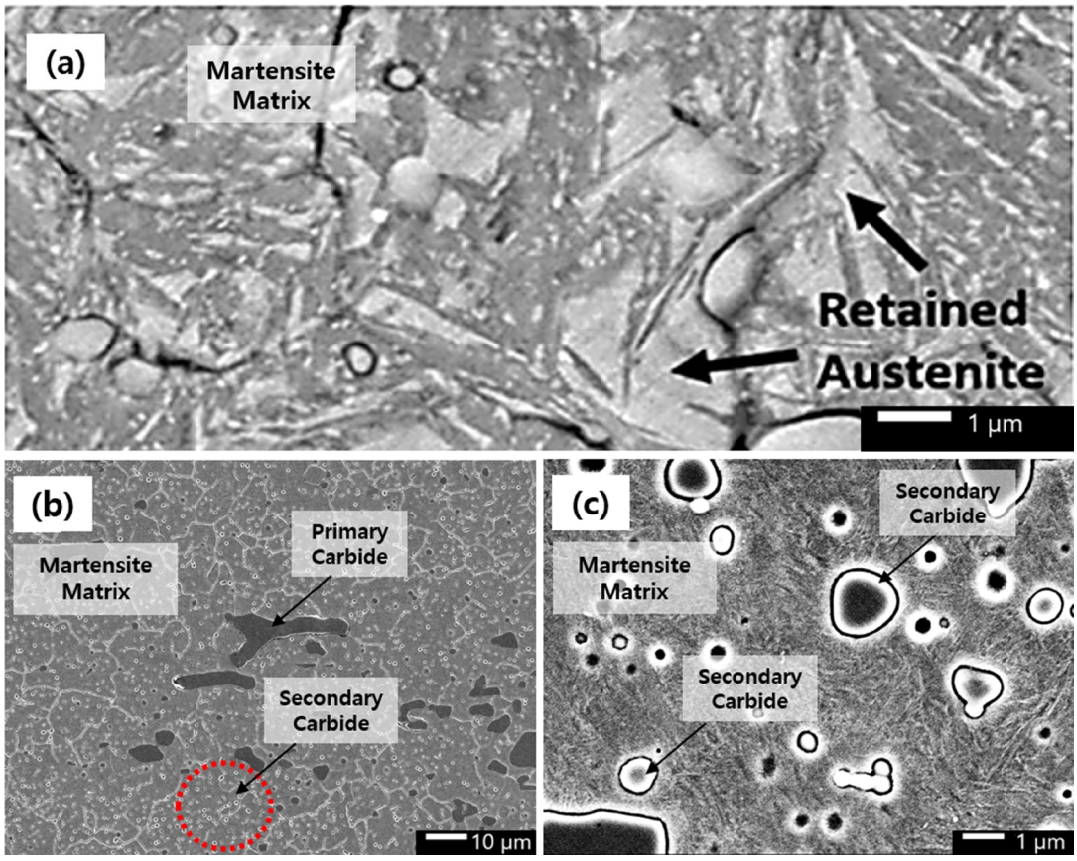

Fig. 1. SEM micrograph of heat treated AISI D2 specimens: (a) Typical surface morphology of retained austenite observed in the martensite matrix [9], (b) Primary and secondary carbides within the martensite matrix of the experimental alloy, and (c) Enlarged micrograph of secondary carbides in the experimental alloy

(SEM). (Fig. 1) To identify the phases present in the specimen microstructures, EDS analysis using SEM was performed in conjunction with a literature review. [10] The types of carbides were not identified, as both primary and secondary carbides act as hard phases. Therefore, rather than analyzing their individual effects, the correlation between microstructure and mechanical properties was more efficiently assessed based on the overall amount and distribution of carbides.

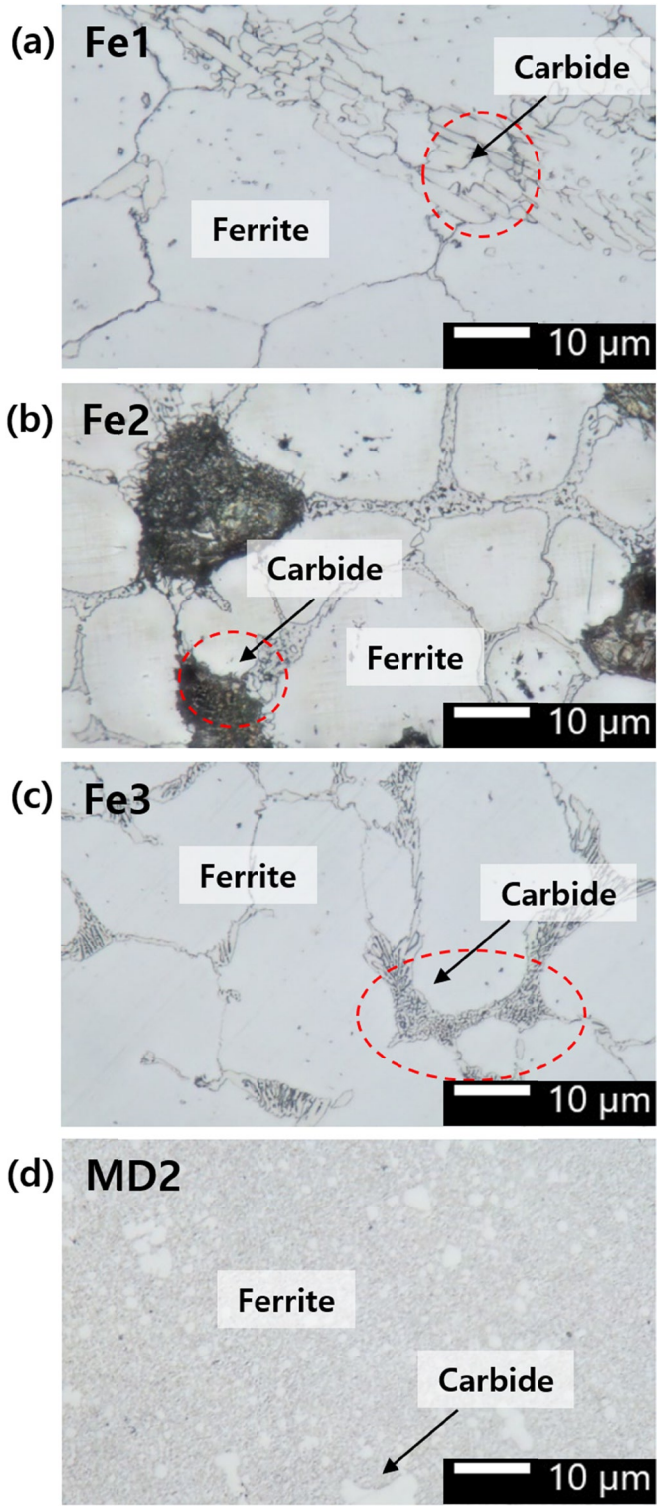

Fig. 2. Optical micrographs of the as-received specimens: (a) Fe1, (b) Fe2, (c) Fe3, and (d) MD2

Hardness testing was performed using a Vickers hardness tester with a load of 0.75 kgf applied for 10 seconds. The reported values represent the average of 15 measurements taken from different locations on each specimen.

3. Results and discussion

To investigate the effects of compositional variation and heat treatment on the microstructure and mechanical properties, modified alloy compositions were prepared, followed by microstructure analysis and hardness testing. The results revealed that mechanical properties are governed not only by the phase fraction, but also by the average size and distribution of each phase.

(Fig. 2) In the case of the as-received specimens, the microstructures of Fe1, Fe2, and Fe3 were observed to be composed of carbides distributed mainly at grain boundaries in the ferrite matrix. MD2 has large carbides distributed unevenly compared to other specimens. (Fig. 5) The average hardness of each specimen is 465 HV for Fe1, 284 HV for Fe2, 393 HV for Fe3, and 287 HV for MD2.

(Fig. 3) In the case of the as-quenched specimens, the microstructure consisted of martensite (M), carbide (C), and a mixed phase of martensite and austenite (M+A). The phase fractions in Fe1 are 43% martensite, 15% carbide, and 42% a mixed phase of martensite and austenite. The average size of each phase is 7.2 μm for martensite, 17.2 μm for carbide. The phase fractions in Fe2 are 30% martensite, 1% carbide, and 69% a mixed phase of martensite and austenite. The average size of each phase is 20.2 μm for martensite, and 36.2 μm for carbide. The phase fractions in Fe3 are 34% martensite, 2% carbide, and 64% a mixed phase of martensite and austenite. The average size of each phase is 5.4 μm for martensite, and 25.9 μm for carbide. The phase fractions in MD2 are 92% martensite, and 8% carbide. The average size of each phase is 0.25 μm for martensite and 9.7 μm for carbide. (Fig. 5) The average hardness values of the as-quenched specimen were 766 HV for Fe1, 826 HV for Fe2, 862 HV for Fe3, and 661 HV for MD2.

(Fig. 4) In the case of as-tempered specimens, the microstructure consisted of tempered martensite (TM), carbide (C), and a mixed phase of tempered martensite and carbide (TM+C). The phase fractions in Fe1 are 52% tempered martensite, 5% carbide, and 43% a mixed phase of tempered martensite and carbide. The average size of each phase is 16 μm for tempered martensite, and 13.4 μm for carbide. The phase fractions in Fe2 are 57% tempered martensite, 8% carbide, and 35% a mixed phase of tempered martensite and carbide. The average size of each phase is 25.3 μm for tempered martensite, 6.4 μm for carbide. The phase fractions in Fe3 are 47% tempered martensite, 8% carbide, and 45% a mixed phase of tempered martensite and carbide. The average size of each phase is 16.6 μm for tempered martensite, and 16.8 μm for carbide. MD2: The phase fractions are 87% tempered martensite, and 13% carbide. The average size of each phase is 0.57 μm for tempered martensite and 2.3 μm for carbide. (Fig. 5) The average hardness values of the as-tempered

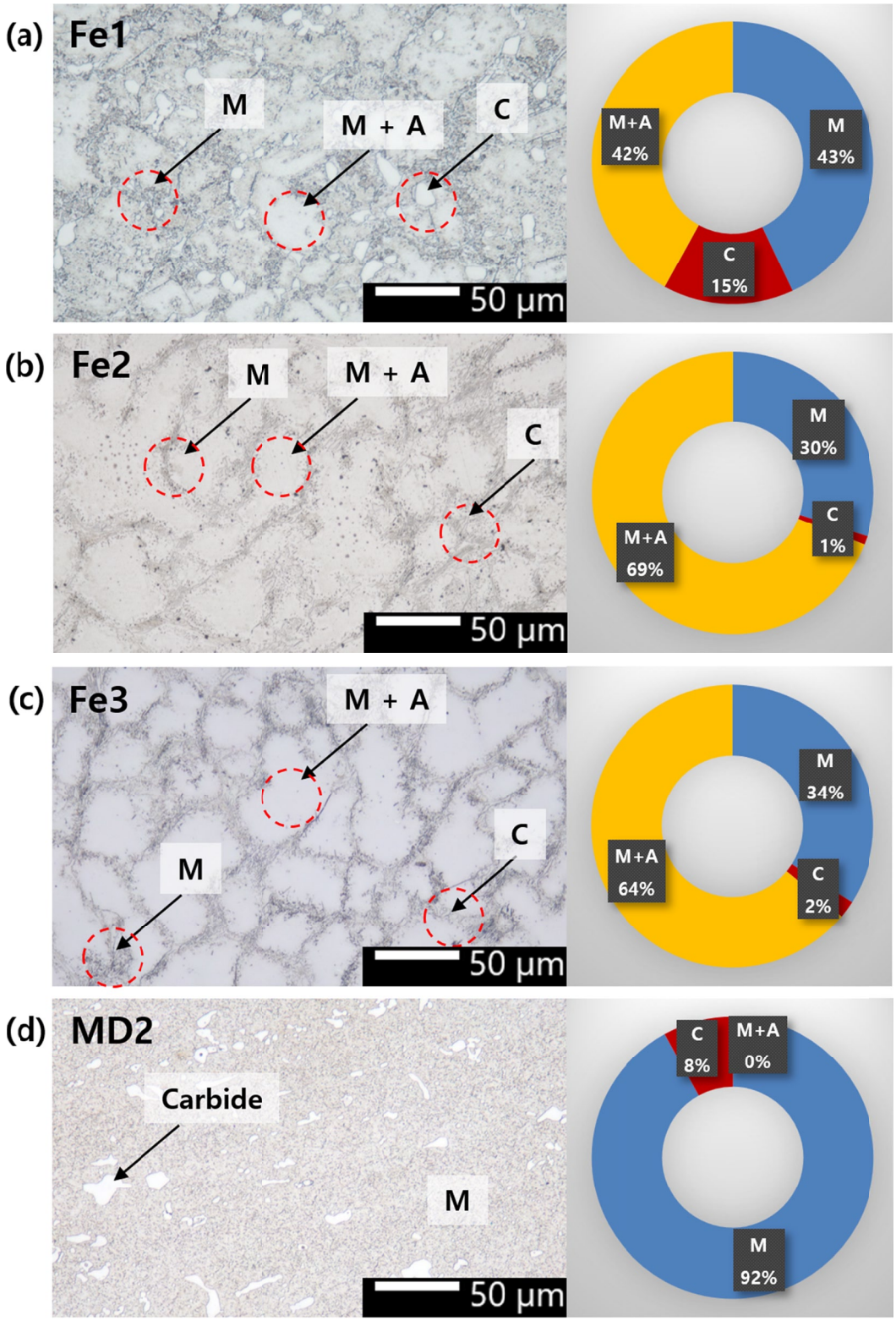

Fig. 3. Surface morphologies and phase fraction(area%) analysis of the quenched specimens: (a) Fe1, (b) Fe2, (c) Fe3, and (d) MD2

specimens were 677 HV for Fe1, 581 HV for Fe2, 712 HV for Fe3, and 605 HV for MD2.

As shown in Figs. 2,3 and 4, carbide phases were primarily distributed along grain boundaries. [11] This grain boundary segregation is attributed to two factors: (1) grain boundaries, as high-energy regions, experience less phase transformation during quenching; and (2) carbon tends to concentrate near these regions. The formation of grain boundary carbides is attributed to the dissolution and re-precipitation behavior during austenitizing and quenching. During austenitizing, incomplete dissolution of carbides and non-uniform diffusion of alloying elements in the matrix can occur. [12] As a result, segregation of elements near grain boundaries can occur, promoting carbide precipitation during subsequent quenching. This localized carbide precipita-

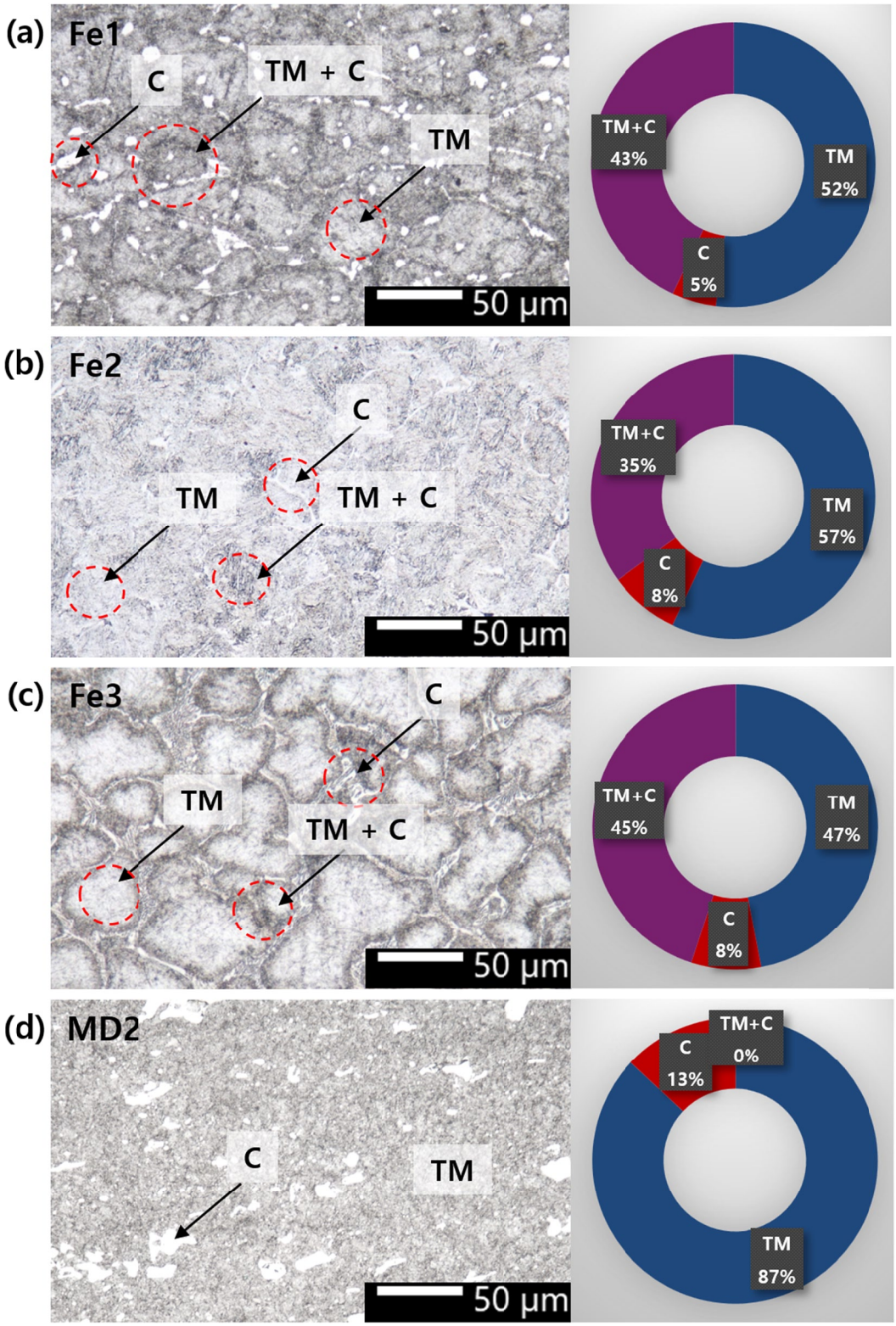

Fig. 4. Surface morphologies and phase fraction(area%) analysis of the tempered specimens: (a) Fe1, (b) Fe2, (c) Fe3, and (d) MD2

tion at grain boundaries significantly affects the surrounding matrix composition and phase transformation behavior. In particular, when carbides are primarily precipitated along grain boundaries, the surrounding matrix retains a relatively high carbon concentration. [13] The elevated C content stabilizes austenite at lower temperatures by increasing its lattice energy, as C atoms are incorporated into the austenite lattice. This local stabilization of austenite can inhibit its transformation into martensite during quenching. Consequently, the formation of grain boundary carbides contributes to an increased amount of the mixed phase of martensite and austenite after heat treatment. Such a structure may interrupt the continuity of the martensite matrix, thereby reducing the overall hardness. However, the relatively high hardness observed in as-quenched Fe2 and Fe3,

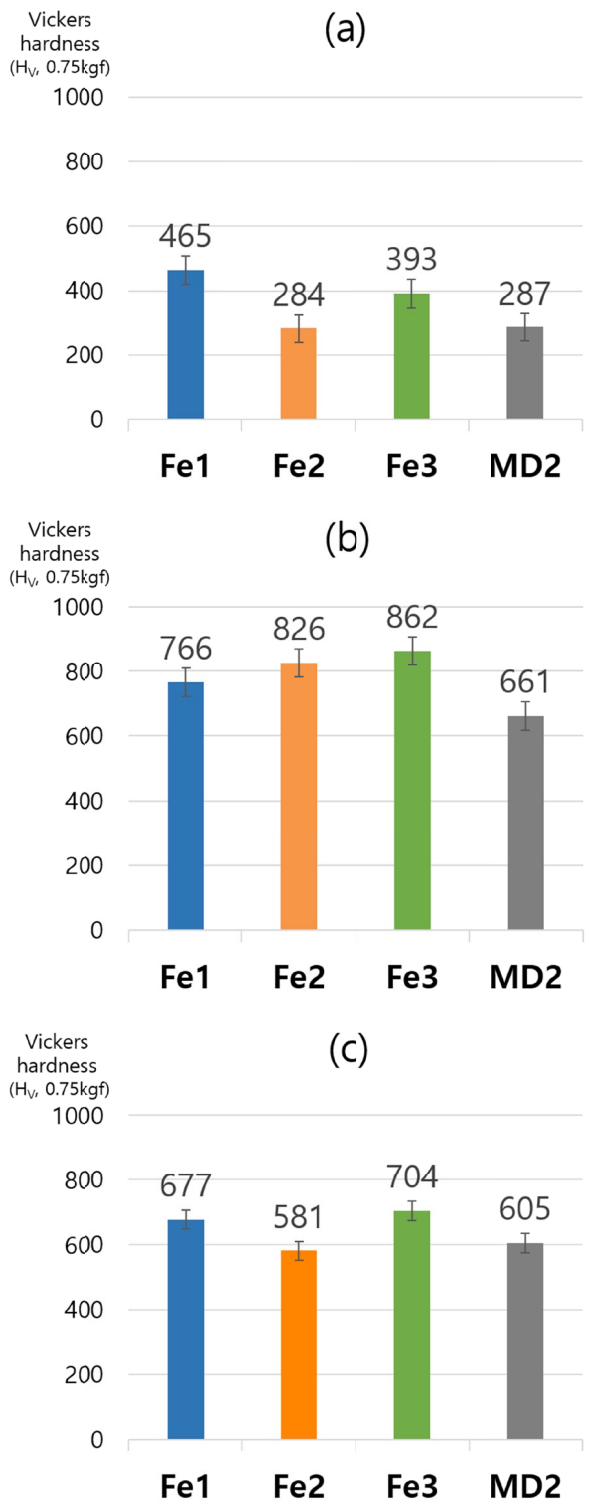

Fig. 5. Comparison of Vickers hardness values of Fe1, Fe2, Fe3 and MD2 in different condition: (a) as-received, (b) as-quenched, and (c) as-tempered specimens

despite their high fraction of mixed phases, is primarily attributed to the precipitation of a large number of carbides during heat treatment – facilitated by the higher Cr and Mo contents in Fe2 and the elevated C and V contents in Fe3.

Among the as-quenched specimens, Fe2 and Fe3 exhibited similar mixed-phase fractions of martensite and austenite – approximately 60%. However, Fe3 showed higher hardness than Fe2. This discrepancy is attributed to two key factors: first, the average size of the carbide phase in Fe2 was 36.2 μm, which is larger than the 25.9 μm observed in Fe3; second, the average martensite size in Fe3 was 5.4μm, significantly smaller than the 20.2 μm in Fe2.

Among the as-tempered specimens, Fe2 exhibited the lowest hardness. Although its higher Mo content may contribute to solid solution strengthening, the effect of reduced V content – leading to a lower amount of fine secondary carbide precipitation – appears to have had a more significant impact on the decreased hardness. Additionally, Fe2 exhibited a larger average size of tempered martensite compared to Fe1 and Fe3. [14] A high fraction of coarsely tempered martensite likely contributed to reduction in hardness. Fe3 showed the highest hardness both before and after tempering, which can be attributed to its higher carbon content. The high C content in Fe3 promoted increased carbide precipitation, which contributed to better hardness retention during tempering. This is supported by the experimental results, as Fe3 exhibited a smaller reduction in hardness compared to Fe2 and showed a higher fraction of mixed phase of tempered martensite and carbide. Tempered MD2 developed a dense structure of fine tempered martensite, which helped limit the reduction in hardness. Nonetheless, the relatively low hardness of MD2 appears to result from a combination of factors, including lower V content and non-uniform carbide distribution.

Overall, while Cr and Mo contents influenced the results to some extent, C and V contents were found to be the most critical factors affecting microstructure and hardness among the experimental specimens.

4. Conclusions

In this study, the alloy compositions and heat treatment conditions of AISI D2-based experimental alloys were systematically designed to experimentally investigate the relationship between microstructure and mechanical properties. By adjusting the contents of key alloying elements, a methodology was proposed for designing compositions that enable the formation of a uniform microstructure while maintaining high hardness. Furthermore, a quantitative analysis of the effects of heat treatment on the microstructure of AISI D2 revealed that alloy composition, as well as the phase fraction, average size, and distribution uniformity of each phase, significantly influence the resulting hardness.

For a more comprehensive understanding of the relationship between the microstructure and mechanical properties of AISI D2 steel, future studies should include mechanical properties evaluations such as tensile testing.

Acknowledgments

This work was supported by the Technology Program No.20024344, ‘Development of Al-Based high carbon steel alloy design and sintering-based

additive manufacturing technology for 7.0L/hr-level high-speed production of powertrain components with tensile strength over 1.0 GPa in the next-generation mobility'.

This work was also supported by the Competency Development Program for Industry Specialists of the Korea Government (MOTIE), operated by Korea Institute for Advancement of Technology (KIAT) (RS-2024-00406598, HRD program, Professional Manpower Education & Training for 3D Printing Industries).

REFERENCES

[1] H.Torkamni, Sh. Raygan, J. Rassizadehghani, Comparing microstructure and mechanical properties of AISI D2 steel after bright hardening and oil quenching. Material & Design **54**, 1049-1055 (2014). DOI: https://doi.org/10.1016/j.matdes.2013.09.043

[2] G. Robert, G. Krauss, R. Kennedy, Tool steels, **5**th ed., ASM International, Materials Park, Ohio (1998).

[3] P.M. Uterweiser, Heat treater's guide: standard practices and procedures for steel. **2**nd ed., AM Soc Met, Ohio (1989), pp. 506-566.

[4] G.E. Totten, Steel heat treatment. **2**nd ed., Taylor & Francis, New York (2006), pp. 214-215.

[5] S.H. Avner, Introduction to physical metallurgy. **2**nd ed., McGraw-Hill, New York (1988), pp. 398-417.

[6] K. Bungrrdt, E. Kunze, E. Hom, Investigation of the structure of the iron-chromium-carbon system. Arch. Eisenttenwes **28** (1958).

[7] P. Moro, S. Gimenez, I. Itrurriza, Sintering behavior and fracture toughness characterization of D2 matrix tool steel: Comparison with wrought and PM D2. Scripta Mater. **46**, 369-373 (2002). DOI: https://doi.org/10.1016.S1359-6462(01)01253-2

[8] S. Kheirandish, H. Saghafian, J. Hedjazi, M. Momeni, Effect of heat treatment on microstructure of modified cast AISI D3 cold work tool steel. J. Iron Steel Res. Int. **17** (9), 40-45 (2010). DOI: https://doi.org/10.1016/S1006-706X(10)60140-9

[9] M.D. Conci, D.M.A. Centeno, H. Goldenstein, P.F.S. Farina, Study of Short Tempering for AISI D2 Cold Work Tool Steel. Mater. Res. **26** (suppl. 1) (2023). DOI: https://doi.org/10.1590/1980-5373-MR-2023-0059

[10] D. Das, A.K. Dutta, K.K. Ray, Correlation of microstructure with wear behavior of deep cryogenically treated AISI D2 steel. Wear **267** (9-10), 1371-1380 (2009). DOI: https://doi.org/10.1016/j.wear.2008.12.051

[11] J.B Papazian, D.N. Besherb, Grain boundary segregation of carbon in iron. Metall. Trans. **2**, 497-503 (1971). DOI: https://doi.org/10.1007/BF02663340

[12] T. Cao, C. Cheng, F. Ye, H. Hv, J. Zhao, et al., Relationship between carbon segregation and the carbide precipitation along grain boundary based on the structural unit model. J. Mater, Sci. **55**, 7883-7893 (2020). DOI: https://doi.org/10.1007/s10853-020-04537-2

[13] X. Qiao, L. Han, W. Zhang, J. Gu, Effect of carbon content on mechanical stability of retained austenite in TRIP-assisted steels. ISIJ Int. **56** (1), 140-147 (2016). DOI: https://doi.org/10.2355/isijinternational.isijint-2015-248

[14] R.A Grange, C.R Hribal, L.F Porter, Hardness of tempered martensite in carbon and low-alloy steels. Metall. Trans. A **8**, 1775-1785 (1977). DOI: https://doi.org/10.1007/BF02646882

[15] Journal of Korean Powder Metallurgy Institute **25** (2), 137-143 (2018). DOI: https://doi.org/10.4150/kpmi.2018.25.2.137